JOURNAL OF AGRICULTURAL AND FOOD CHEMISTRY

Salt Effect on the pH Profile and Kinetic Parameters of Microbial Phytases

ABUL H. J. ULLAH,* KANDAN SETHUMADHAVAN, AND EDWARD J. MULLANEY

Southern Regional Research Center, Agricultural Research Service, U.S. Department of Agriculture, 1100 Robert E. Lee Boulevard, New Orleans, Louisiana 70124

The pH profiles of two microbial phytases were determined using four different general purpose buffers at different pH values. The roles of calcium chloride, sodium chloride, and sodium fluoride on activity were compared in these buffers. For *Aspergillus niger* phytase, calcium extended the pH range to 8.0. A high concentration of sodium chloride affected the activity of fungal phytase in the pH 3–4 range and shifted the pH optimum to 2.0 from 5.5 in *Escherichia coli* phytase. As expected, both of the microbial phytases were inhibited by sodium fluoride at acidic pH values. Because the K_m for phytate increased nearly 2-fold for fungal phytase while V_{max} increased about 75% in a high concentration of sodium chloride, it is possible that salt enhanced the product to dissociate from the active site due to an altered electrostatic environment. Modeling studies indicate that while the active site octapeptide's orientation is very similar, there are some differences in the arrangements of α-helices, β-sheets, and coils that could account for the observed catalytic and salt effect differences.

KEYWORDS: Phytase; histidine acid phosphatase (HAP); substrate specificity site (SSS); histidine acid phytase (Haphy)

INTRODUCTION

Among the members of the acid phosphatase class of enzymes, several histidine acid phosphatases (HAP) have been identified with a high specific activity for phytic acid (*1*). To designate the HAPs that can readily accommodate phytate as a substrate, Oh and co-workers have proposed the term histidine acid phytase or HAPhy (*2*). This research was spawned by the need for an efficient phytase that could be utilized as an animal feed additive. Phytic acid is the primary phosphate storage compound in most plant seeds and grains (*3*). The increased use of soybean and other plant meals in animal feed (*4*) created a need for a phytase that would allow monogastric animals, swine, poultry, etc., which lack an effective phytase in their digestive system, to utilize the phosphates that are esterified to myo-inositol, a six-carbon sugar. At this time, all of the available commercial phytases for this animal feed application belong to the subclass HAP.

Previous studies have demonstrated that the effectiveness of *Aspergillus niger* phytase as an animal feed additive could be enhanced by site-directed mutagenesis (*5*). Specific changes in the amino acids residues composing the enzyme's substrate specificity site (SSS) resulted in a pH profile optimized for the actual conditions in the animal's stomach.

While various plant phytases have been reported, none possessed the high specific activity and other desirable catalytic traits such as pH optima, stability, etc. found in the microbial phytases. For this reason, comparatively little research has been conducted on plant phytases. Recently, the gene for lily pollen was cloned (*6*) and its product was further characterized. Initial studies of lily pollen phytase had shown it to have a pH optimum of 8.0 and to be described in the literature as an alkaline phytase. The recent finding that lily pollen phytase shared the same catalytic mechanism common to HAP was therefore unexpected.

In this study, the buffer system and salt used in the characterization of lily pollen phytase was employed to modify the pH profile of two microbial phytases. The ability of sodium chloride to simulate the effect of specific SSS mutants that abolished the dip in the typical bihump profile of pH optima was observed. This fact supports the notion that the electrostatic environment of the SSS components, which is key to substrate binding at a specific pH, could be altered by high salt concentration and thus mimic the effect caused by the mutation of a "gate keeper" residue. The salt did not help the fungal phytase to catalyze phosphomonoesterase activity beyond pH 7. Calcium, however, extended the pH curve to 8.0 with only 10% of the peak activity at pH 5.5.

MATERIALS AND METHODS

Source of Phytase. *A. niger* phytase was obtained from Gist Brocade (Delft, The Netherlands), which is the recombinant product of the *A. niger* (*ficuum*) NRRL 3135 phyA gene. *Escherichia. coli* phytase, *appA2* gene product, was a gift from Phytex LLC (Portland, Maine), which was overexpressed in the gene of *Pichia pastoris* (*8*).

Purification of Phytase. We have purified the recombinant fungal phytase using sequential ion-exchange columns Macroprep S and Q columns (*7*). The purified phytase had an approximate specific activity

* To whom correspondence should be addressed. Tel: 504-286-4365. Fax: 504-286-4367. E-mail: abul.ullah@ars.usda.gov.

10.1021/jf073137i
Published on Web 04/10/2008

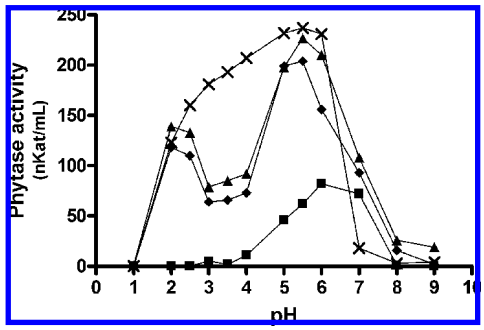

Figure 1. pH vs activity profile of *Aspergillus niger* phytase (phyA) in the presence of 10 mM sodium fluoride (■), 1 mM calcium chloride (▲), 500 mM sodium chloride (×), and no additive (♦). The buffers used were glycine (pH 1.0–3.0), acetate (pH 3.5–5.5), and imidazole (pH 6.0–9.0).

of 3500 nKat/mg of protein and showed a single band on sodium dodecyl sulfate−polyacrylamide gel electrophoresis (data not shown). For the purification of appA2 phytase, the crude culture filtrate was dialyzed against 25 mM glycine-HCl, pH 2.8, buffer and loaded onto a MacroPrep S column and eluted as a single activity component in a linear salt 0–0.5 M sodium chloride gradient. The final specific activity of the phytase was about 15000 nKat/mg of protein at 55 °C.

Phytase Assay. Both the fungal and the bacterial phytases were assayed in 1.0 mL volume at 37 °C in 50 mM sodium acetate (assay buffer) at pH 5.5 with 750 nmol of sodium phytate as described previously (*9*). The liberated inorganic ortho-phosphates were quantitated spectrophotometrically using a freshly prepared AMA reagent consisting of acetone, 10 mM ammonium molybdate, and 5.0 N sulfuric acid (2:1:1, v/v). Adding 2.0 mL of AMA solution per assay tube terminated the phytase assay. After 30 s, 0.1 mL of 1.0 M citric acid was added to each tube. The absorbance was read at 355 nm after blanking the spectrophotometer with an appropriate control. Values were expressed as nKat/mL. A Kat (katal) is defined as mole of substrate converted per second.

Choice of Buffers. In this study, the phytase activity was measured at various pH values (1.5−9) using different buffers such as 25 mM glycine-HCl (pH 1.5–3.0), 50 mM sodium acetate (3.5–5.5), and 25 mM imidazole (6–9). The phytase activity was also measured using a Tris-maleate system (pH 5.5–9.0).

Michaelis Constant (K_m) and V_{max} Determination. The K_m and V_{max} were determined at 37 °C using an increasing concentration of sodium phytate from 10 to 1000 μM. WindowChem's software Enzyme Kinetics version 1.1 was used to compute both the K_m and the V_{max} values.

Molecular Modeling. Molecular graphics images were produced using the UCSF Chimera package (version 1) from the Resource for Biocomputing, Visualization, and Informatics at the University of California, San Francisco (*10*). Two Protein Data Bank (PDB) files, 1ihp (*11*) and 1dko (*12*), representing fungal and bacterial phytase, respectively, were downloaded from the RCSB PDB Web site (http://www.rcsb.org/pdb/home/home.do).

RESULTS

Effect of Ions on *A. niger* PhyA Phytase. The fungal phytase activity was measured in the presence of 10 mM sodium fluoride, a known inhibitor of HAP, 1 mM calcium chloride, and 500 mM sodium chloride at various pH values using glycine-HCl, sodium acetate, and imidazole buffers. The results are shown in **Figure 1**. The typical bihump pH profile, which is characteristic of *A. niger* PhyA phytase, was realized in the absence of any ions. The pH profile of the enzyme in presence of calcium chloride also showed this bihump profile. The calcium ion boosted the activity about 20% at both pH 2.0 and pH 5.0 and allowed the biocatalyst to cleave phosphate at pH 8 and 9, but the activity was only about 12% of the peak activity at pH 5.0 (**Figure 1**).

Sodium fluoride, a known inhibitor of acid phosphatase, abolished activity at pH 1.5−3.5 while inhibiting about 70% activity at pH 6.0. The inhibitor seemed to be less effective at pH range of 4.5−6.5.

Sodium chloride at a 500 mM concentration not only boosted the activity from pH 1.5 to 6.0 but also abolished the dip at pH 2.5−4. To probe whether the K_m for phytate was lowered to enhance the activity, we determined the Lineweaver–Burk plot at pH 4.0 and 5.0. The results are shown in **Table 1**. The Michaelis constant (K_m) for phytate nearly doubled by the salt while the V_{max} increased from 75 to 166%. However, the kinetic perfection did decrease in both of the cases due to doubling of the K_m. When potassium chloride was used in place of sodium salt, the K_m increased 6-fold while the V_{max} increased 2-fold (data not shown).

The effects of ions were also investigated in Tris-maleate buffer (pH 5.5−9). It was observed that 10 mM sodium fluoride inhibited the activity but more so at pH 5−6.5. The other ions, calcium and sodium, did not, however, significantly increase the activity. At the alkaline pH range, the phytase catalyzed the breakdown of phytate at 15–20% level as compared to what it did at pH 5.5 (**Figure 2**). This level of catalysis at alkaline pH is much higher than what was observed, typically 5–6% of the peak activity, when imidazole buffer was used (**Figure 1**).

Effect of Ions on *E. coli appA2* Phytase. Similar to fungal phytase the *E. coli* phytase was severely inactivated by 10 mM sodium fluoride from pH 1.5 to 6.0. However, at pH 7, the enzyme was inhibited about 85%. Unlike the fungal phytase, the salt effect was negative for the *E. coli* phytase. Sodium chloride at 500 mM did not inhibit the activity at pH 2−2.5, but at pH 3 and above, it severely inhibited the activity; the salt effect was more pronounced at pH 5−7. The calcium ion at 1 mM boosted the activity about 10–15% throughout the entire pH range, 1.5−7 (**Figure 3**).

In Tris-maleate buffer (pH 5.5), sodium fluoride severely inhibited the *appA2* phytase activity in the entire pH range (**Figure 4**). Sodium chloride (500 mM) also inactivated the bacterial phytase in a similar fashion. Unlike the fungal enzyme, calcium ion did not increase the activity throughout the entire pH range. Furthermore, no discernible activity peak was observed in the alkaline pH range. The enzyme typically catalyzed only 5% of the peak activity in the alkaline pH range (**Figure 4**).

The K_m for phytate was nearly doubled by 500 mM sodium chloride at pH 2.5 while the activity was lowered about 10% (**Table 1**). The kinetic parameters of *appA2* phytase under similar salt environments at pH 6.0 could not be determined because the Lineweaver–Burk plot gave a negative K_m value. The severe inhibition of phosphohydrolase activity effectuated by the high concentration of salt may have caused this anomaly. The same aberrance was noticed when we used 250 and 125 mM salt to determine the K_m of bacterial phytase at pH 6.0 (data not given).

Modeling of the Active Site. Figure 5A,B shows a computer-deduced three-dimensional structure of fungal phyA and bacterial appA2 phytase, respectively. The active site region where the heptapeptide (RHGXRXP) and HD motif is located is circled by a red elliptical boundary. The active site residues are shown in ball and stick configuration. Both the fungal and the bacterial phytase belong to phosphoglycerate mutaselike superfamily of proteins and members of the HAP family. Therefore, the overall structure of these phytases shows some similarity, especially the arrangements of α-helices and β-sheets.

Table 1. Kinetic Properties of Fungal and Bacterial Phytase in the Presence and Absence of 0.5 M NaCl at 37 °C

phytase	assay condition	K_m (μM)	V_{max} (nkat/mg)	turnover number (TON) (s^{-1})	kinetic perfection TON/K_m (s^{-1} M^{-1})
fungal	pH 5.0; no salt	33	8469	745	2.25×10^7
	pH 5.0; 0.5 M NaCl	88	14827	1305	1.48×10^7
	pH 4.0; no salt	36	4418	389	1.08×10^7
	pH 4.0; 0.5 M NaCl	57	11788	1037	1.82×10^7
bacterial	pH 2.5; no salt	72	22669	1167	1.62×10^7
	pH 2.5; 0.5 M NaCl	121	20582	1060	0.87×10^7
	pH 6.0; No salt	200	36019	1857	0.92×10^7
	pH 6.0; 0.5 M NaCl	*a*	*a*	*a*	*a*

[a] Cannot be accurately determined due to severe inactivation.

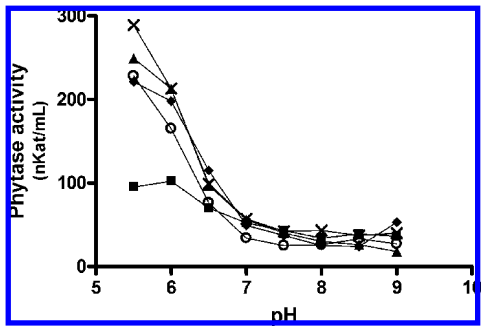

Figure 2. pH vs activity profile of *Aspergillus niger* phytase (phyA) in 100 mM Tris-maleate buffer system in the presence of 10 mM sodium fluoride (■), 1 mM calcium chloride (▲), 500 mM sodium chloride (×), all of the additives (○), and no additive (♦).

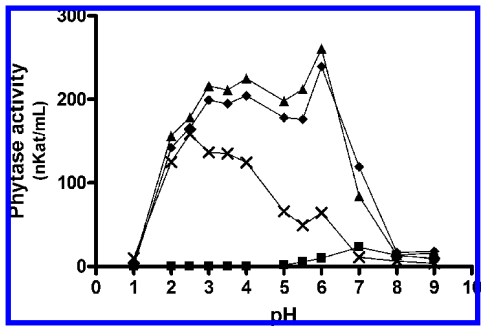

Figure 3. pH vs activity profile of *E. coli* phytase (appA2) in the presence of 10 mM sodium fluoride (■), 1 mM calcium chloride (▲), 500 mM sodium chloride (×), and no additive (♦). The buffers used were glycine (pH 1.0–3.0), acetate (pH 3.5–5.5), and imidazole (pH 6.0–9.0).

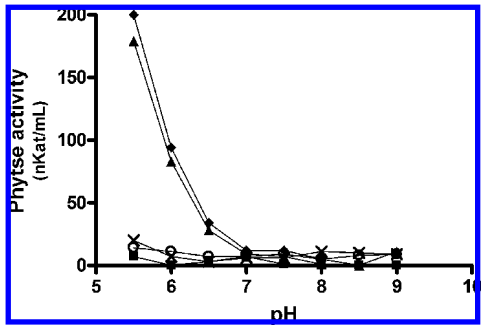

Figure 4. pH vs activity profile of *E. coli* phytase (appA2) in 100 mM Tris-maleate buffer system in the presence of 10 mM sodium fluoride (■), 1 mM calcium chloride (▲), 500 mM sodium chloride (×), all of the additives (○), and no additive (♦).

However, the active site heptapeptide, which forms a coil, shows 75% sequence homology. The HD dipeptide, which is also an integral part of the active center of phytase, comes from an α-helix and is placed very close to R58 of fungal phytase and R16 of bacterial phytase. The bacterial phytase is 42 amino acids shorter from the N-terminal end as compared to the fungal phytase; nonetheless, they both form an identical β-sheet that engenders a coil on which the active site heptapeptide is located. The three-dimensional models of both of the phytases reveal other structural differences. For example, the two short antiparallel β-sheets left to the C terminus, which are present in appA2 phytase, were absent in phyA phytase (**Figure 5A**,**B**).

DISCUSSION

Previous studies have demonstrated that the pH profile of HAPhys can be altered by choice of buffer (*13*) or by site-directed mutagenesis to change specific amino acid residues that compose the enzyme's SSS (*5*). Site-directed mutagenesis of the SSS of *A. niger* phytase has been shown to alter the enzyme's pH profile to match the pH environment in the stomach of swine. Feed trials in swine have recently documented the effectiveness of this technology to optimize the phytase activity for this application (*5*). This study has established that both of the pH profiles for *A. niger* and *E. coli* phytase can be modified by both a buffer, Tris-maleate, and by the introduction of salts, sodium chloride and calcium chloride.

The addition of sodium chloride enhanced activity over the pH range of 1.5−6.0 in fungal phytase. Like the SSS mutations in previous studies (*5, 13*), a significant increase in activity between 2.5 and 5.0 was realized by the addition of 500 mM sodium chloride. In the SSS mutations, the increased activity in this range was attributed to a more favorable electrostatic environment that accelerated the hydrolysis of phytate by the enzyme's catalytic mechanism. On the basis of the Michaelis constant (K_m) presented in **Table 1**, sodium chloride appears to have an effect on the binding of the substrate to the active site; the K_m was doubled. The observed higher activity is probably due to accelerated exit of the leaving group (inorganic ortho-phosphate) after cleavage of the phosphomonoester bond. In *E. coli* phytase, 500 mM sodium chloride depressed the activity over the pH range of 1.5−7.0. Therefore, it appears that the electrostatic environment at the active center of bacterial phytase is markedly different from its fungal counterpart. Because both *A. niger* and *E. coli* are HAPhy and share the same heptapeptide active-site sequence, some other structural component, such as differences in amino acids composing their SSS, appears to be involved in their response to high salt.

It has not escaped our attention that there is a parallel between the effect of a single mutation in the substrate-binding domain of the fungal phytase (*5*) and high salt in abolishing the dip in activity in the pH range 3.0−4.0. In the first case, the electrostatic environment was changed by a genetic approach; in the second case, the high salt also resulted in the same change. While it will be detrimental to change the electrostatic environ-

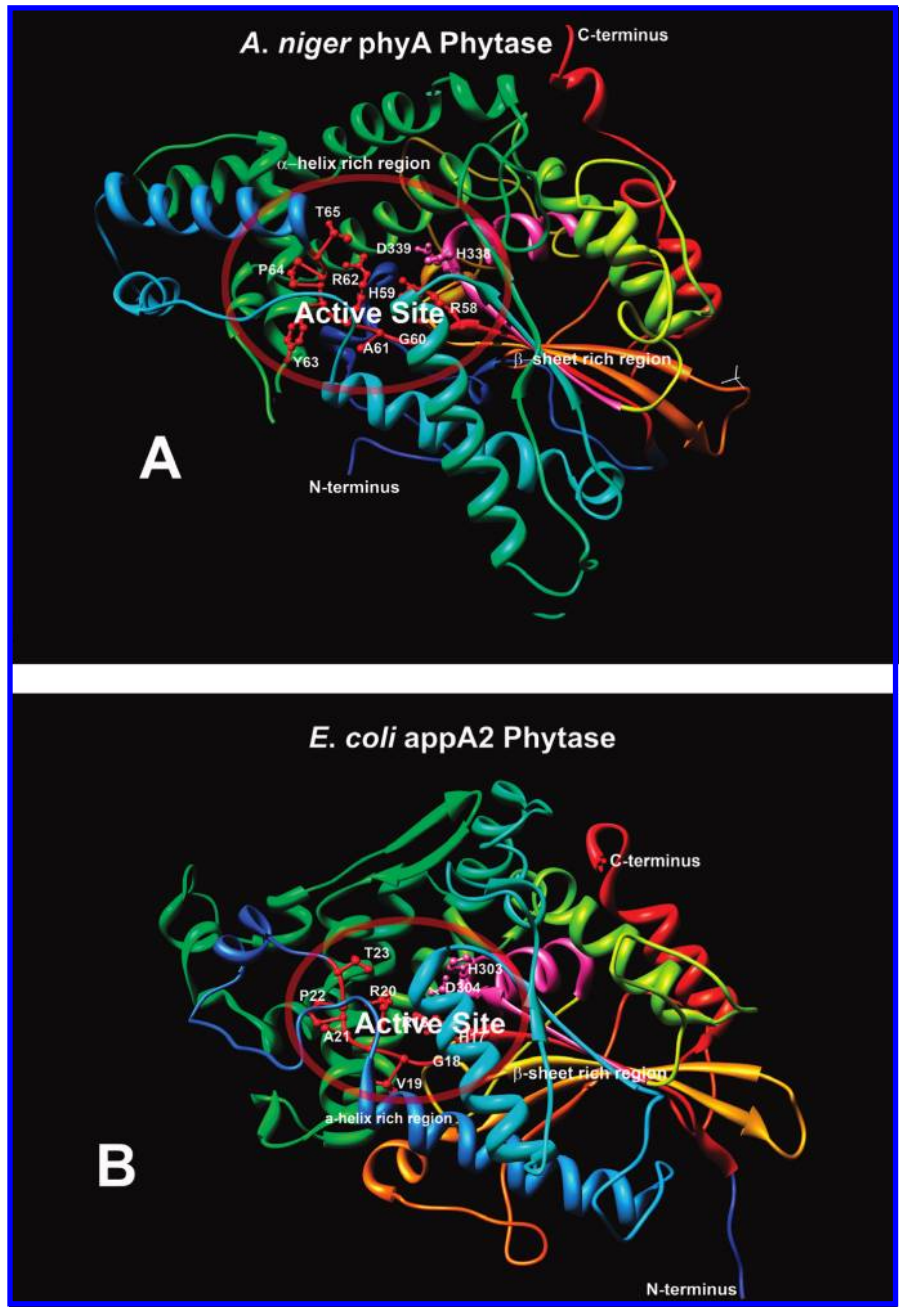

Figure 5. Computer-assisted three-dimensional structure of *A. niger* phyA phytase (**A**) and *E. coli* appA2 phytase (**B**). The red elliptical boundary shows the active site heptapeptide region and the "HD" motif, a hallmark of the HAP family of enzymes.

ment of the stomach of the animal by salt to boost phytase's activity at pH 3.0−4.0, a genetic approach would be more realistic. Even though phytase's kinetic efficiency is very high (**Table 1**), the enzyme could be tailor-made to perform even better at stomach pH; the results of the high salt effect on V_{max} of fungal phytase presented in this paper gives us this optimism from a scientific perspective. A comparative molecular modeling study between the fungal and the bacterial phytase had indicated that despite the active site similarity the two phytases differ in the arrangements of α-helices, β-sheets, and coils. The low molecular activity (turnover number) of the fungal phytase could be enhanced by borrowing structural elements from appA2; therefore, a knowledge-based structural refinement in fungal phytase based on bacterial phytase has a promising future vis-à-vis its catalytic rate enhancement. The results of this study support the notion that additional knowledge-based modification of the phyA molecule could further enhance its catalytic efficiency.

LITERATURE CITED

(1) Mullaney, E. J.; Ullah, A. H. J. The term phytase comprises several different classes of enzymes. *Biochem. Biophys. Res. Commun.* **2003**, *312*, 179–184.

(2) Oh, B. C.; Choi, W. C.; Park, S.; Kim, Y. O.; Oh, T. K. Biochemical properties and substrate specificities of alkaline and histidine acid phytases. *Appl. Microbiol. Biotechnol.* **2004**, *63*, 362–372.

(3) Wodzinski, R. J.; Ullah, A. H. J. Phytase. *Adv. Appl. Microbiol.* **1996**, *42*, 263–302.

(4) Rumsey, G. L. Fishmeal and alternate sources of protein in fish feeds: Update 1993. *Fisheries* **1993**, *18*, 14–19.

(5) Kim, T.; Mullaney, E. J.; Porres, J. M.; Roneker, K. R.; Crowe, S.; Rice, S.; Ko, T.; Ullah, A. H. J.; Daly, C. B.; Lei, X. G. Shifting the pH Profile of *Aspergillus niger* PhyA Phytase to match the stomach pH enhances its effectiveness as an animal feed additive. *Appl. Environ. Microbiol.* **2006**, *72*, 4397–4403.

(6) Mehta, B. D.; Jog, S. P.; Johnson, S. C.; Murthy, P. P. N. Lily pollen alkaline phytase is a histidine phosphatase similar to mammalian multiple inositol polyphosphate phosphatase (MINPP). *Phytochemistry* **2006**, *67*, 1874–1886.

(7) Ullah, A. H.; Sethumadhavan, K.; Mullaney, E. J.; Ziegelhoffer, T.; Austin-Phillips, S. Characterization of recombinant fungal phytase (*phyA*) expressed in tobacco leaves. *Biochem. Biophys. Res. Commun.* **1999**, *264*, 201–206.

(8) Rodriquez, E.; Han, Y.; Lei, X. G. Cloning, sequence, and expression of an *Escherichia coli* acid phosphatase/phytase gene (appA2) isolated from pig colon. *Biochem. Biophys. Res. Commun.* **1999**, *257*, 117–123.

(9) Ullah, A. H. J.; Gibson, D. M. Extracellular phytase (E.C. 3.1.3.8) from *Aspergillus ficuum* NRRL 3135: Purification and characterization. *Prep. Biochem.* **1987**, *17*, 63–91.

(10) Pettersen, E. F.; Goddard, T. D.; Huang, C. C.; Couch, G. S.; Greenblatt, D. M.; Meng, E. C.; Ferrin, T. E. UCSF Chimera—A visualization system for exploratory research and analysis. *J. Comput. Chem.* **2004**, *25*, 1605–1612.

(11) Kostrewa, D.; Gruninger-Leitch, F.; D'Arcy, A.; Broger, C.; Mitchell, D.; van Loon, A. P. Crystal structure of phytase from *Aspergillus ficuum* at 2.5 A resolution. *Nat. Struct. Biol.* **1997**, *4*, 185–190.

(12) Lim, D.; Golovan, S.; Forsberg, C. W.; Jia, Z. Crystal structures of *Escherichia coli* phytase and its complex with phytate. *Nat. Struct. Biol.* **2000**, *7*, 108–113.

(13) Mullaney, E. J.; Daly, C. B.; Kim, T.; Porres, J. M.; Lei, X. G.; Sethumadhavan, K.; Ullah, A. H. J. Site-directed mutagenesis of *Aspergillus niger* NRRL 3135 phytase at residue 300 to enhance catalysis at pH 4.0. *Biochem. Biophys. Res. Commun.* **2002**, *297*, 1016–1020.

Received for review October 25, 2007. Revised manuscript received February 12, 2008. Accepted February 26, 2008. Mention of trade names or commercial products in this publication is solely for the purpose of providing specific information and does not imply recommendation or endorsement by the U.S. Department of Agriculture.

JF073137I